PHYSICAL REVIEW B

CONDENSED MATTER AND MATERIALS PHYSICS

THIRD SERIES, VOLUME 57, NUMBER 22 1 JUNE 1998-II

RAPID COMMUNICATIONS

Rapid Communications are intended for the accelerated publication of important new results and are therefore given priority treatment both in the editorial office and in production. A Rapid Communication in **Physical Review B** *may be no longer than four printed pages and must be accompanied by an abstract. Page proofs are sent to authors.*

Microscopic study of oxygen-vacancy defects in ferroelectric perovskites

C. H. Park and D. J. Chadi

NEC Research Institute, 4 Independence Way, Princeton, New Jersey 08540

(Received 22 September 1997)

We investigate the nature of atomic relaxations around oxygen-vacancy defects in the ferroelectric perovskite $PbTiO_3$ through first-principles pseudopotential total energy calculations. A tail-to-tail polarization is one of the patterns that emerges from atomic relaxations around oxygen vacancies and its stability is found to be enhanced by charge trapping. Oxygen vacancies in Ti-O-Ti chains along the polarization axis are more favorable than those in Ti-O-Ti planes normal to the axis. The possible role of oxygen vacancies in fatigue and aging is discussed. [S0163-1829(98)50522-X]

Ferroelectric materials are now the focus of intense study because of the advantages they confer in making dynamical and nonvolatile memory components.[1] Ferroelectric thin films made from lead zirconate titanate (PZT) and strontium bismuth tantalate have been extensively investigated since they exhibit high remnant polarizations, suitable coercive fields, and high resistance. The wide commercialization of ferroelectric based devices has been hampered, by problems such as fatigue, aging, and imprinting.[1–3] Fatigue denotes the degradation of remnant polarization with repetitive switching cycles while aging indicates polarization degradation with time in a poled capacitor.[1,2] Imprinting occurs when a series of electric pulses with the same sign makes it harder to reverse the ''imprinted'' polarization.[2,3]

Fatigue and aging affect the lifetime of ferroelectric based devices and have been extensively investigated. Although the underlying mechanisms for these complicated phenomena are not yet well understood, defects, particularly electrically charged ones, are known to play an important role. The effect on fatigue of domain pinning,[4] charged defects,[5–8] grain boundaries, ferroelectric-electrode interfaces,[9,10] and of extended defect sheets have been examined in several studies.[1,2,7,11] High quality films recently fabricated by using metal oxide electrodes with a low concentration of defects have shown much improved lifetimes and fatigue properties.[12]

Defects affect various properties of ferroelectrics such as the remnant polarization, motion of domain walls, dielectric constant, and leakage current. Among various defects, oxygen vacancies are thought to be the most mobile and abundant in perovskite ferroelectrics.[13] There are several indications that oxygen vacancies play an essential role in polarization degradation phenomena such as fatigue and aging.[2,11,13,14] Their complexing with impurities and other defects may also be responsible for imprint phenomena.[2,3] However, the microscopic properties of oxygen vacancies and the precise manner in which they affect bulk properties have not been examined in detail yet.

The main objective of this study is an examination of the atomic structure of oxygen-vacancy defects and defect-induced polarization changes in the prototypical perovskite ferroelectric $PbTiO_3$ thorough first-principles calculations. These types of calculations have only recently been applied to the study of ferroelectric materials.[15–22] The approach has been successful in explaining the microscopic mechanisms of spontaneous polarization,[15–19] phase diagrams,[19,20] and 180° domain boundaries[21] in a number of perovskites systems. King-Smith and Vanderbilt have greatly stimulated theoretical research in this area by devising a procedure[22] from which the change in macroscopic polarization and Born effective charges resulting from a lattice distortion can be obtained from a knowledge of the wave functions.[18,19,22]

We choose $PbTiO_3$ because its phase diagram is simple and because results derived for it are expected to be qualitatively valid for PZT and other simple perovskite structures. $PbTiO_3$ has a high temperature paraelectric cubic phase and

a lower temperature tetragonal ferroelectric phase. The first-principles pseudopotential method[23,24] used in our calculations is based on the local density approximation (LDA).[25] Norm-conserving nonlocal pseudopotentials[26] were generated by the scheme of Troullier and Martins (TM),[27] and Kleinman-Bylander type of fully separable pseudopotentials were constructed.[28] The semicore $5d$ electrons of Pb and the $3s$ and $3p$ electrons of Ti were included in the calculations and the $3s$ potential was chosen as the local one for Ti. Hamann has previously shown that p- or d-local potentials for Ti do not adequately describe the Ti-O bonding.[29] The calculated lattice constant for the cubic structure is 3.91 Å, which is about 2% smaller than the experimental value of 3.97 Å,[30] and is in good agreement with previous theoretical results.[20,22] For the simulation of defects, we employ various supercell geometries with 40 to 60 atoms per cell.

Defect-induced lattice deformations can modify local fields and polarization patterns in ferroelectrics. Our results demonstrate quantitatively the way in which neutral and $+2$ charged oxygen vacancies along Ti-O-Ti chains normal to and along the polarization axis affect the bonding and polarization patterns on a microscopic scale. We find that hole capture or electron ionization at a vacancy enhances the atomic relaxations around a vacancy and, for some configurations, leads to the creation of an antiphase polarization. Such vacancy-induced antiphase polarizations can play an important role in domain pinning and polarization degradation.

In the low temperature tetragonal phase, $PbTiO_3$ has a large c/a ratio of 1.063.[30] The Ti atoms in O-Ti-O chains along the c axis move parallel to the axis, alternately strengthening and weakening the Ti-O bonds along the axis. The strong bonds result from a hybridization between Ti($3d$) and O($2p$) orbitals.[15,16] Although $PbTiO_3$ is an ionic material, the tetragonal phase has mixed covalent and ionic bonding character. The calculated bond lengths of 1.8 Å for the dimerized and 2.4 Å for the decoupled Ti-O bonds are in very good agreement with the corresponding experimental values of 1.78 Å and 2.38 Å.[30] The transition from the cubic to the ferroelectric tetragonal phase is found to be accompanied by an energy reduction of 0.24 eV per 5 atom unit cell, consistent with earlier theoretical results.[15] The ferroelectric phase resulting from Ti-O coupling is satisfactorily described, therefore, by a pseudopotential approach. In the following we examine the effect of oxygen-vacancy defects on Ti-O bonding and polarization for the tetragonal phase of $PbTiO_3$.

Two types of oxygen atoms can be distinguished in tetragonal $PbTiO_3$: those in dimerized Ti-O-Ti chains along the c axis [O(1)] and those in Ti-O-Ti chains along the a and b axes normal to the c axis [O(2)]. Unlike O(1) atoms, O(2) atoms are bonded to *two* Ti atoms in zigzag O-Ti-O chains [see Fig. 1(a)]. The two distinct oxygen sites O(1) and O(2) can give rise, therefore, to two types of oxygen-vacancy defects: (i) a missing O(1) atom along a c axis represented here by V_c, and (ii) an O(2) vacancy in the a-b plane denoted by V_{ab}.

We, first, examine the atomic displacements of Ti, O, and Pb atoms closest to a V_c type of an oxygen vacancy using a periodic 40 atom ($2a\times2a\times2c$) tetragonal cell. Oxygen vacancies in $PbTiO_3$ are double donor defects. The nearest two

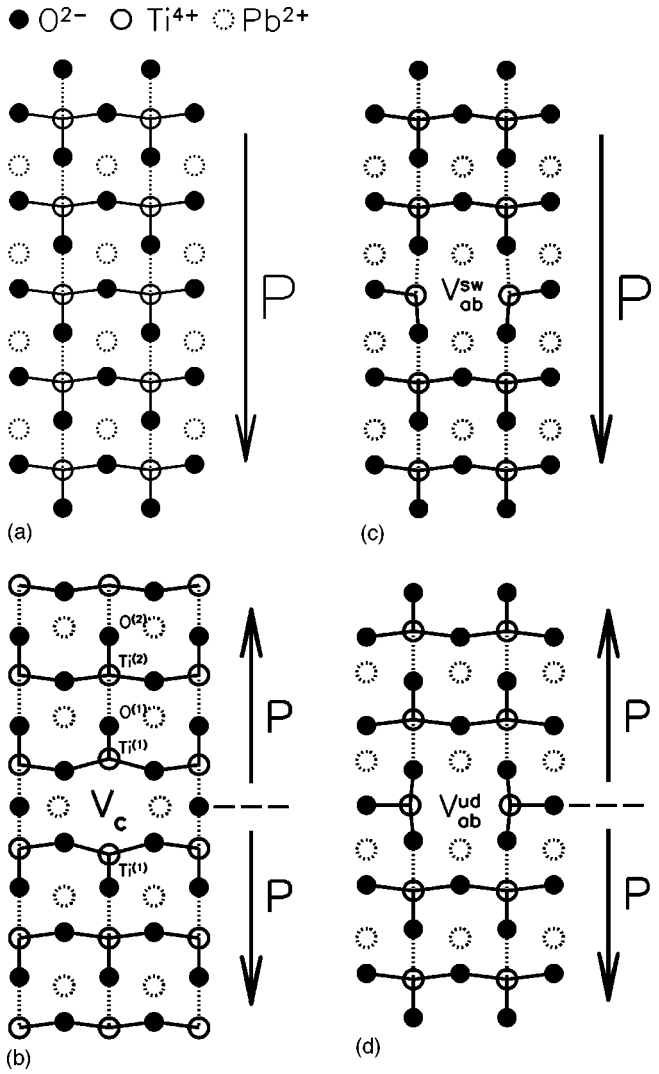

FIG. 1. Schematic atomic structures for (a) tetragonal phase of $PbTiO_3$, (b) oxygen vacancy V_c, (c) oxygen vacancy V_{ab}^{sw}, and (d) oxygen vacancy V_{ab}^{ud}. Pb atoms (dashed circles) are located on a different plane.

Ti^{+4} and four Pb^{+2} cations of a $+2$ charged V_c defect are displaced away from it while the nearest eight O^{-2} anions are attracted towards it. The directions of these displacements can be simply inferred from the Coulombic interaction of a positively charged defect center with its neighboring atoms. The atomic relaxations around a V_c-type oxygen vacancy defect, are shown in Fig. 1(b). As discussed below, the relaxations give rise to a tail-to-tail polarization pattern around the vacancy.

The magnitudes of the displacements from ideal tetragonal positions of the nearest neighbor Ti, O, and Pb atoms for V_c^{2+} are, respectively, 0.21 Å, 0.04 Å, and 0.16 Å. The displacements are smaller in the neutral charge state (V_c^0) where the Ti, O, and Pb atoms move by 0.17 Å, 0.02 Å, and 0.06 Å. The contour graphs of the electronic charge density for the donor state of V_c for two different planes are shown in Figs. 2(a) and 2(b). The donor state is strongly localized around the nearest-neighbor Ti atoms. In the neutral state, where the donor level is doubly occupied, there is a reduced repulsive interaction between the vacancy and neighboring cations resulting in smaller relaxations.

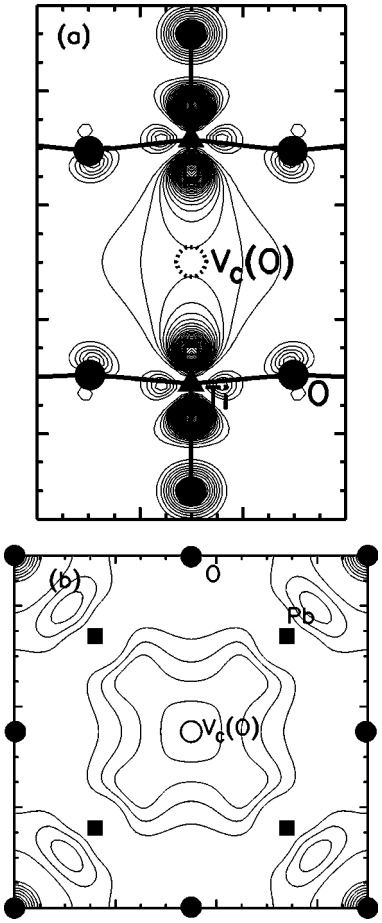

FIG. 2. Contours of electron density of the donor state of the V_c type of oxygen vacancy; (a) on a Ti-O-Ti plane and (b) on a Pb-O plane. The contour spacings are in units of 5 electrons per 40 atom cell. Filled circles, triangles, and boxes describe the location of oxygen, Ti, and Pb atoms, respectively, and open circles indicate the location of oxygen vacancies.

For V_{ab}-type oxygen vacancies in the ab plane of the tetragonal phase we find two structures characterized by distinctly different Ti-O couplings and polarization patterns along the c axis as shown in Figs. 1(c) and 1(d). The polarization around the vacancy is either in the same direction as the bulk polarization [Fig. 1(c)] or there is a tail-to-tail geometry [Fig. 1(d)]. In the following discussions we denote the two V_{ab} configurations in Figs. 1(c) and 1(d) as V_{ab}^{sw} (for ''switchable'') and V_{ab}^{ud} for ''up-down'' based on their induced polarization patterns.

The magnitudes of atomic displacements in V_{ab} type defects are found to be similar to those for V_c. A comparison of the total energies for V_c and V_{ab}^{ud} indicates that V_c is nearly 0.3 eV more stable. The Ti atoms in V_{ab} do not relax as fully as those in V_c because of tetragonal lattice strain, increasing the energy of this state. The energy of V_{ab}^{sw} relative to V_{ab}^{ud} cannot be reliably estimated from our calculations. The energies of head-to-head domain walls that occur when using a periodic supercell for V_{ab}^{ud} or for V_c need to be determined before we can make an energy comparison. We expect, however, that V_{ab}^{sw} is the lower energy state, especially at high electric fields.

We have investigated defect-induced polarization changes by examining Ti-O bonding patterns around oxygen-vacancy defects, employing a rod shaped supercell of 50 atoms with (1,1,0), $(\bar{1},1,0)$, (0,0,5) lattice vectors. From the Ti-O bonding geometry and atomic displacements we find that V_c induces a ''tail-to-tail'' type of polarization pattern, as shown in Fig. 1(b). The atomic displacement pattern has mirror symmetry around the vacancy with $Ti^{(1)}$ atoms away from the vacancy and coupling to $O^{(1)}$ atoms. This results in a new pattern of short and long Ti-O bonds that *propagates* along the c axis. The ''bond lengths'' for the coupled Ti-O pairs are estimated to be 1.76 Å while the distance between the decoupled $O^{(1)}$ and $Ti^{(2)}$ atoms are 2.12 Å for the $V_c^{2+}(O)$ state. These Ti-O distances are similar to the 1.72 Å and 2.33 Å values in the ideal ferroelectric phase.

Atomic arrangements in the ferroelectric phase of perovskites show a displacive behavior and the correlation length of the polarization has been suggested to be about 10–50 nm along the c axis and 1–2 nm along the a and b direction, leading to a needle shaped correlation volume.[31] We expect a similar, needle shaped, up-down polarization pattern for the V_c^{2+} vacancy. Polarization along the a or b axes is suppressed because of strain in the tetragonal phase. For an up-down polarization pattern, one component becomes embedded in the bulk polarization and, as a result, an *antiphase* polarization is induced by the vacancy. Needlelike antiphase domains oriented along the c axis have been observed at surfaces and at imperfections.[32–34]

For the ''switchable'' V_{ab}^{sw} state in Fig. 1(c) the coupling and decoupling of Ti-O pairs can be done coherently with the bulk and in this case no antiphase polarization is generated. The polarization around the vacancy together with the bulk polarization can be reversed by the application of an electric field. A V_{ab}^{sw} defect, therefore, does not affect the bulk polarization as much as a V_c defect. Vacancy migration and the gradual transformation of V_{ab}^{sw} into V_c may play a role in the degradation of switchable polarization and give rise to aging.

Positively charged carriers tend to accumulate around the tails of antiphase polarization domains to compensate the polarization charges resulting from the abrupt change in polarization and to stabilize these domains.[9] The stabilization of antiphase domains through charge trapping at defects such as oxygen vacancies results in a decrease of the switchable polarization and contributes to aging. A transformation of V_{ab}^{sw} into the more stable V_c state also contributes to a degradation of the switchable polarization. At sufficiently low temperatures, the barrier for oxygen diffusion prevents this transformation and only charge capture becomes the dominant mechanism for aging. It has been suggested that aging may be a consequence of a preexisting oxygen-vacancy population.[14]

Domain pinning is a major factor in fatigue and can occur as a result of defect agglomeration.[7] The pinning effect from a single oxygen vacancy is small. The area and energy of a tail-to-tail domain wall is minimized by a planar accumulation of charged defects, such as V_c-type vacancies, lying normal to the polarization axis. Our results which are based on small unit cells are in this regime of a planar arrangement of defects. The gradual formation of a defect sheet of V_c oxygen vacancies leads to strong pinning of an up-down do-

main wall and can be a major contributor to fatigue.[7,5] This picture is supported by Pan, Yue, and Tuttle's finding that in fatigued PZT ceramics the nonfatigued initial polarization properties are largely recovered when the direction of the applied field is rotated by 90° with respect to the direction of the initial field.[6] In the rotated state, the electric field lies in the plane of the charged defects (at least initially) and these defects do not influence the energetics of polarization switching. The rotation of the field direction turns the V_c-type vacancies into V_{ab} defects. As these new defects migrate to form V_c-type planar defects normal to the new electric field axis, fatigue develops once more.

In summary, we have examined three types of oxygen-vacancy defects and their effects on local Ti-O bonding and polarization in $PbTiO_3$. The results of our calculations indicate that oxygen vacancies are one possible source of domain pinning and polarization fatigue in $PbTiO_3$. The pinning effect is maximized for a planar arrangement of oxygen vacancies, especially when the vacancies lie in Ti-O-Ti chains along the *c* axis. The migration of charged oxygen vacancies from Ti-O-Ti chains in the *ab* plane into the energetically more favorable sites in Ti-O-Ti chains along the *c* axis can contribute to aging.

[1] J. F. Scott and C. A. P. Araujo, Science **246**, 1400 (1989).
[2] W. L. Warren, D. Dimos, and R. M. Waser, Mater. Res. Bull. **21**, 40 (1996).
[3] T. Mihara, H. Watanabe, and C. A. Paz de Araujo, Jpn. J. Appl. Phys., Part 1 **32**, 4168 (1993).
[4] A. Gruverman, O. Auciello, and H. Tokumoto, Appl. Phys. Lett. **69**, 3191 (1996).
[5] W. L. Warren, B. A. Tuttle, and D. Dimos, Appl. Phys. Lett. **67**, 1426 (1995).
[6] W. Y. Pan, C. F. Yue, and B. A. Tuttle, Ceram. Trans. **625**, 385 (1992).
[7] C. Brennan, Ferroelectrics **150**, 199 (1993).
[8] T. Mihara, H. Watanabe, and C. A. P. Araujo, Jpn. J. Appl. Phys., Part 1 **33**, 5281 (1994).
[9] W. L. Warren, D. Dimos, B. A. Tuttle, R. D. Nasby, and G. E. Pike, Appl. Phys. Lett. **65**, 1018 (1994).
[10] I. K. Yoo and S. B. Desu, Mater. Sci. Eng., B **13**, 319 (1992).
[11] H. M. Duiker, P. D. Beal, J. F. Scott, C. A. P. Araujo, B. M. Melnice, J. D. Cuchiro, and L. D. McMillan, J. Appl. Phys. **68**, 5783 (1990).
[12] C. K. Kwok, D. P. Vijay, S. B. Desu, N. r. Parikh, and E. A. Hill, Integr. Ferroelectr. **3**, 121 (1993); T. Nakamura, Y. Nakao, A. Kamisawa, and H. Takasu, Appl. Phys. Lett. **65**, 1522 (1994).
[13] D. M. Smyth, Ferroelectrics **116**, 117 (1991); Annu. Rev. Mater. Sci. **15**, 329 (1985); M. V. Raymond and D. M. Smyth, J. Phys. Chem. Solids **57**, 1507 (1996).
[14] V. M. Gurevich, *Electric Conductivity of Ferroelectrics* (Israel Program for Scientific Translations, Jerusalem, 1971), p. 306.
[15] R. E. Cohen, Nature (London) **358**, 136 (1992).
[16] R. Resta, M. Posternak, and A. Baldereschi, Phys. Rev. Lett. **70**, 1010 (1993).
[17] R. D. King-Smith and D. Vanderbilt, Phys. Rev. B **49**, 5828 (1994).
[18] R. Yu and H. Krakauer, Phys. Rev. Lett. **74**, 4067 (1995).
[19] W. Zhong, R. D. King-Smith, and D. Vanderbilt, Phys. Rev. Lett. **72**, 3618 (1994); W. Zhong, D. Vanderbilt, and K. M. Rabe, *ibid.* **73**, 1861 (1994).
[20] U. V. Waghmare and K. M. Rabe, Phys. Rev. B **55**, 6161 (1997).
[21] J. Padilla, W. Zhong, and D. Vanderbilt, Phys. Rev. B **53**, R5969 (1996).
[22] R. D. King-Smith and D. Vanderbilt, Phys. Rev. B **47**, 1651 (1993); **48**, 4442 (1993).
[23] M. L. Cohen, Phys. Scr. **T1**, 5 (1982).
[24] J. Ihm, A. Zunger, and M. L. Cohen, J. Phys. C **12**, 4409 (1979).
[25] P. Hohenberg and W. Kohn, Phys. Rev. **136**, B864 (1964); W. Kohn and L. J. Sham, Phys. Rev. **140**, A1133 (1965).
[26] D. R. Hamann, M. Schlüter, and C. Chiang, Phys. Rev. Lett. **43**, 1494 (1979).
[27] N. Troullier and J. L. Martins, Phys. Rev. B **43**, 1993 (1991).
[28] L. Kleinmann and D. M. Bylander, Phys. Rev. Lett. **48**, 1425 (1982).
[29] D. R. Hamann, Phys. Rev. B **56**, 14 979 (1997).
[30] *Landolt-Börnstein Tables*, edited by K.-H. Hellwege and A. M. Hellwege (Springer, Berlin, 1969).
[31] M. E. Lines and A. M. Glass, *Principles and Applications of Ferroelectrics and Related Materials* (Clarendon, Oxford, 1977), p. 525.
[32] W. J. Merz, Phys. Rev. **95**, 690 (1954).
[33] K. Amanuma, T. Hase, and Y. Miyasaka, Jpn. J. Appl. Phys., Part 1 **33**, 5211 (1994).
[34] W. H. Shepherd, in *Ferroelectric Thin Films*, edited by E. R. Myers and A. I. Kingon, MRS Symposia Proceedings No. 200 (Materials Research Society, Pittsburgh, 1990), p. 277.